

Effect of surface plasmon coupling with radiating dipole on the polarization characteristics of AlGaN-based light-emitting diodes

Yi Li(李毅), Mei Ge(葛梅), Meiyu Wang(王美玉), Youhua Zhu(朱友华), and Xinglong Guo(郭兴龙)

Citation: Chin. Phys. B, 2022, 31 (**7**): 077801. DOI: 10.1088/1674-1056/ac4cbb
Journal homepage: http://cpb.iphy.ac.cn; http://iopscience.iop.org/cpb

What follows is a list of articles you may be interested in

Improving the performance of a GaAs nanowire photodetector using surface plasmon polaritons

Xiaotian Zhu(朱笑天), Bingheng Meng(孟兵恒), Dengkui Wang(王登魁), Xue Chen(陈雪), Lei Liao(廖蕾), Mingming Jiang(姜明明), and Zhipeng Wei(魏志鹏)
Chin. Phys. B, 2022, 31 (**4**): 047801. DOI: 10.1088/1674-1056/ac1e15

High-efficiency reflection phase tunable metasurface at near-infrared frequencies

Ce Li(李策), Wei Zhu(朱维), Shuo Du(杜硕), Junjie Li(李俊杰), and Changzhi Gu(顾长志)
Chin. Phys. B, 2021, 30 (**5**): 057802. DOI: 10.1088/1674-1056/abe9a6

Quantum plasmons in the hybrid nanostructures of double vacancy defected graphene and metallic nanoarrays

Rui Tang(唐睿), Yang Xu(徐阳), Hong Zhang(张红), and Xin-Lu Cheng(程新路)
Chin. Phys. B, 2021, 30 (**1**): 017804. DOI: 10.1088/1674-1056/abaedb

Acoustic plasmonics of Au grating/Bi_2Se_3 thin film/sapphirehybrid structures

Weiwu Li(李伟武), Konstantin Riegel, Chuanpu Liu(刘传普), Alexey Taskin, Yoichi Ando, Zhimin Liao(廖志敏), Martin Dressel, Yuan Yan(严缘)
Chin. Phys. B, 2020, 29 (**6**): 067801. DOI: 10.1088/1674-1056/ab8a3c

Processes underlying the laser photochromic effect in colloidal plasmonic nanoparticle aggregates

A E Ershov, V S Gerasimov, I L Isaev, A P Gavrilyuk, S V Karpov
Chin. Phys. B, 2020, 29 (**3**): 037802. DOI: 10.1088/1674-1056/ab6551

Effect of surface plasmon coupling with radiating dipole on the polarization characteristics of AlGaN-based light-emitting diodes

Yi Li(李毅)†, Mei Ge(葛梅), Meiyu Wang(王美玉), Youhua Zhu(朱友华), and Xinglong Guo(郭兴龙)

School of Information Science and Technology & Tongke School of Microelectronics, Nantong University, Nantong 226019, *China*

(Received 18 October 2021; revised manuscript received 3 January 2022; accepted manuscript online 19 January 2022)

The optical polarization characteristics of surface plasmon (SP) coupled AlGaN-based light emitting diodes (LEDs) are investigated theoretically by analyzing the radiation recombination process and scattering process respectively. For the $Al_{0.5}Ga_{0.5}N/Al/Al_2O_3$ slab structure, the relative intensity of TE-polarized and TM-polarized spontaneous emission (SE) rate into the SP mode obviously depends on the thickness of the Al layer. The calculation results show that TM dominated emission will be transformed into TE dominated emission with the decrease of the Al thickness, while the emission intensities of both TE/TM polarizations will decrease significantly. In addition, compared with TM polarized emission, TE polarized emission is easier to be extracted by SP coupling. For the $Al_{0.5}Ga_{0.5}N/Al$ nano-particle structure, the ratio of transmittance for TE/TM polarized emission can reach ~ 3.06, while for the Al free structure, it is only 1.2. Thus, the degree of polarization of SP coupled LED can be improved by the reasonable structural design.

Keywords: surface plasmon, AlGaN-based light emitting diodes, FDTD, K-P method

PACS: 78.66.Fd, 78.67.De, 78.67.–n, 78.67.Pt **DOI:** 10.1088/1674-1056/ac4cbb

1. Introduction

AlGaN-based light emitting diodes (LEDs) as the deep ultraviolet (DUV) light sources have attracted great attention due to their potential applications in water purification, optical catalysis and other fields.[1] Although great progress has been made in the research of AlGaN-based DUV LEDs,[2] the luminous efficiency is still lower than that of GaN-based visible LEDs.[3] One of the limiting factors to improve the luminous efficiency of DUV-LEDs is the poor light extraction efficiency (LEE). Different from GaN material, the crystal-field split-off hole (CH) band of AlGaN alloy will become the topmost valence subband with the increase of Al-content,[4] which will lead to the transverse-magnetic (TM) dominated emission.[5] The TM polarization denotes that the emission polarization is perpendicular to the *c*-plane. For *c*-plane AlGaN-based LEDs, TM polarized emission is difficult to extract from the top or bottom surface. In addition, due to the low conductivity of p-AlGaN, the p-GaN contact layer is often employed in AlGaN-based DUV-LEDs, which will lead to strong absorption and reduce the LEE of the device.[6]

In order to improve the performance of DUV LEDs, structural design strategies are often used, such as ultrathin GaN/AlN multiple quantum well (MQW) structure[7] and lateral-polarity structure.[8] Moreover, an alternative method is to adopt the surface plasmon (SP) coupled LED structure, which can enhance both the internal quantum efficiency (IQE) and LEE.[9] For example, He *et al.* reported that the IQE and LEE of DUV LED with Al nanoparticles (NPs) on SiO_2 dielectric interlayer were increased by 230% and 13%, respectively.[10] Interestingly, Zhang *et al.* reported that the enhancement ratio of transverse-electric (TE) mode was larger than that of TM mode through local SP (LSP) coupling,[11] which will help to improve the luminous efficiency of *c*-plane LED devices. The TE polarization denotes that the polarization is parallel to the *c*-plane. The corresponding mechanism was considered that the LSP–QW coupling results in the conversion of some TM emission to TE emission. However, detailed theoretical analysis is lacking in the literature.

In this study, we focus on the effect of SP coupling on the polarization characteristics of DUV LEDs by numerical calculation. Firstly, considering the valence band mixing effects and the scattering relaxation, the TE/TM polarized spontaneous emission (SE) rate into the SP mode are calculated by 6×6 K-P method.[12] The corresponding band structure is obtained by self-consistent solution of Schrödinger–Poisson equations. Then, the scattering process of radiating dipole with TE mode or TM mode in the metal nanostructures is investigated by the three-dimensional (3D) finite-difference time-domain (FDTD) simulation. Thus, the effect of the radiative recombination by SP–QW coupling and the scattering by metal nanostructures on the TE/TM polarized emissions can be described, respectively. Through these simulation results, the influence of SP coupling behavior on the optical anisotropy of AlGaN-based LEDs can be better understood.

2. Theory

When an electron-hole pair in the AlGaN QW is located within the SP fringing field penetration depth, the radiative recombination energy can be transferred into the SP mode instead of into the free space.[13] The corresponding SE rate into the SP mode can be expressed as[12]

†Corresponding author. E-mail: liyi2016@ntu.edu.cn

© 2022 Chinese Physical Society and IOP Publishing Ltd

$$r_1^{\text{spon}}(\hbar\omega) = N(\hbar\omega)\frac{2\pi e^2}{\hbar\omega^2 m_0^2}\frac{2}{L_z}\sum_{\sigma}\sum_{n}\sum_{m}\int_0^{\infty}\left\{\frac{k_t\,\mathrm{d}k_t}{2\pi}|\boldsymbol{E}\cdot\boldsymbol{p}_{nm}^{\sigma}|^2\frac{\Gamma/\pi}{[E_{\sigma,nm}^{\text{cv}}(k_t)-\hbar\omega]^2+\Gamma^2}f_c^n(1-f_v^{\sigma m})\right\}, \tag{1}$$

where L_z is the active layer thickness, k_t is the in-plane wave vector, Γ is the line-width, $\boldsymbol{E}$ is the normalized electric field of surface plasmon polariton (SPP) mode, $E_{\sigma,nm}^{\text{cv}}(k_t)$ is the transition energy from nth conduction sub-band to mth valence sub-band, f_c^n and $f_v^{\sigma m}$ are the Fermi–Dirac distribution function. The density of state (DOS) $N(\hbar\omega)$ of SPP mode for an in-plane metal/dielectric structure can be written as[12]

$$N(\hbar\omega) = \frac{2\pi k_{\text{sp}}\,\mathrm{d}k_{\text{sp}}}{(2\pi)^2\,\mathrm{d}\hbar\omega}L^2. \tag{2}$$

Here, k_{sp} and L^2 are the real part of wave vector and the in-plane area, respectively. As taking account to ohmic loss of metal materials, the DOS of SPP mode will be broadened.[14] The modified DOS can be expressed as

$$N^*(\hbar\omega) = \int N(\hbar\omega_k)\times\frac{\omega_k/2\pi Q_k}{[(\omega-\omega_k)^2+(\omega_k/2Q_k)^2]}\,\mathrm{d}\omega_k, \tag{3}$$

where k and Q_k are the wave vector of SPP mode and quality factor, respectively. The quality factor can be calculated by $Q_k = \omega_k/\alpha v_g$. Here α and v_g are the energy decay rate and group velocity, which can be expressed as $\alpha = 2\,\text{Im}(k)$ and $v_g = \mathrm{d}w_k/\mathrm{d}(\text{Re}(k))$, respectively.[14]

For TE polarized emission, the momentum matrix element $|\boldsymbol{E}\cdot\boldsymbol{p}_{nm}^{\sigma}|^2$ in formula (1) can be written as[12]

$$\begin{aligned}|\boldsymbol{E}\cdot\boldsymbol{p}_{nm}^{\sigma}|^2 &= \left|-\frac{\alpha^*}{\sqrt{2}}\langle S|p_x|x\rangle\langle\phi_n|E_x|g_m^{(1)}\rangle+\frac{\beta}{\sqrt{2}}\langle S|p_x|x\rangle\langle\phi_n|E_x|g_m^{(2)}\rangle\right|^2 \quad \text{for} \quad \sigma = U,\\ &= \left|-\frac{\alpha^*}{\sqrt{2}}\langle S|p_x|x\rangle\langle\phi_n|E_x|g_m^{(4)}\rangle+\frac{\beta}{\sqrt{2}}\langle S|p_x|x\rangle\langle\phi_n|E_x|g_m^{(5)}\rangle\right|^2 \quad \text{for} \quad \sigma = L.\end{aligned} \tag{4}$$

Meanwhile, for TM polarized emission, the momentum matrix element is

$$\begin{aligned}|\boldsymbol{E}\cdot\boldsymbol{p}_{nm}^{\sigma}|^2 &= \left|\beta^*\langle S|p_z|z\rangle\langle\phi_n|E_z|g_m^{(3)}\rangle\right|^2 \quad \text{for} \quad \sigma = U,\\ &= \left|\beta^*\langle S|p_z|z\rangle\langle\phi_n|E_z|g_m^{(6)}\rangle\right|^2 \quad \text{for} \quad \sigma = L.\end{aligned} \tag{5}$$

Here α and β can be obtained by $\alpha = \frac{1}{\sqrt{2}}\exp(\mathrm{i}(\frac{3\pi}{4}+\frac{3\phi}{2}))$ and $\beta = \frac{1}{\sqrt{2}}\exp(\mathrm{i}(\frac{\pi}{4}+\frac{\phi}{2}))$. The azimuthal angle in the k_x–k_y plane is $\phi = \tan^{-1}(k_y/k_x)$. In the calculation, the momentum matrix elements are averaged in azimuth. E_x and E_z are the two components of the normalized electric field in the x and z directions.[12] And the block-diagonalized Hamiltonian is employed for calculating the valence band structure and the wave functions $g_m^{(v)}$ ($v = 1, 2, 3, 4, 5$, and 6).[15] The index σ denotes 3×3 upper (U) and lower (L) Hamiltonians. The single band effective mass Hamiltonian is used for obtaining the conduction band structure and the wave functions ϕ_n.[15]

In order to investigate the scattering process of SP mode in metal nanostructures, the transmission spectrum of SP coupled LED is calculated by 3D FDTD simulation. Figure 1 shows the schematic illustration of simulated structure. A cylindrical Al NP with diameter of 170 nm is placed on the $Al_{0.5}Ga_{0.5}N$ layer. Considering the surface oxidation of Al NP, a 3 nm-thickness Al_2O_3 layer is coated on the surface of Al NP. The dielectric constant ($\varepsilon = \varepsilon_1 + \mathrm{i}\varepsilon_2$) of $Al_{0.5}Ga_{0.5}N$ is calculated by using model dielectric function (MDF).[16] The corresponding critical point (CP) parameters is taken from the fit-determined MDF parameters in Ref. [16]. Thus, the wavelength dependent complex refractive index (n) can be obtained by the formula $n = \sqrt{\varepsilon}$. The real part ε_1 and imaginary part ε_2 of the dielectric constants of $Al_{0.5}Ga_{0.5}N$, Al and Al_2O_3 are shown in Fig. 2. The dielectric constants of Al and Al_2O_3 are taken from the FDTD Solutions software. The radiation dipoles are placed directly below the Al NP. The distance between the dipole and the metal is set to 25 nm. The dipole type is set to electric dipole. The x-axis and z-axis dipoles represent TE and TM dipoles. The dipole power can be calculated by using a box of power monitors (monitor 2 in Fig. 1) around the dipole source. And the transmission power is also obtained by monitor 1. In the calculation, the transmittance of TE/TM modes is defined as the ratio of the transmission power and the dipole power. The perfectly matched layer (PML) boundary conditions are employed on all sides. For the x, y and z directions, the size of the simulation range is 1 μm×1 μm×1 μm.

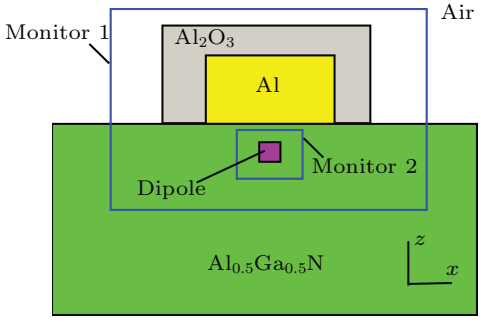


Fig. 1. Schematic illustration of simulated structure.

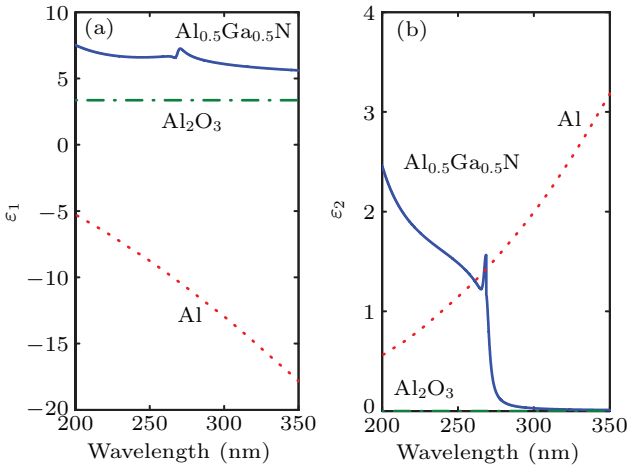


Fig. 2. The real part ε_1 (a) and imaginary part ε_2 (b) of the dielectric constants of $Al_{0.5}Ga_{0.5}N$, Al and Al_2O_3.

3. Results and discussion

3.1. DOS and normalized electric field of SPP mode

Figure 3 shows the schematic diagram of the $Al_{0.5}Ga_{0.5}N$/Al/Al_2O_3 slab structure and the dispersion relation of SPP modes with different Al thickness. The dispersion relation of the SPP mode is calculated by performing a parameter sweep over the wave vector k_{sp} and looking for frequencies with strong resonances. In the calculation, the two-dimensional (2D) FDTD simulation is used. The dimension of the simulation range is 2 μm×1 nm for the z and x directions. The PML boundary condition is set in the z direction and the Bloch boundary condition is set in the x direction. Ten randomly oriented dipoles are set in the simulation region.

In Figs. 3(b) and 3(c), two SPP modes from the AlGaN/Al and Al/Al_2O_3 interfaces can be observed. In the regime of small wave vectors k_{sp}, the dispersion curves from the AlGaN/Al interface are close to the light lines, and the waves can extend into the dielectric space. Therefore, SPPs are known as Sommerfeld–Zenneck waves in this regime.[17] In the regime of large wave vectors, the SPP mode from the AlGaN/Al interface approaches the SP "resonance" energy ($E_{SP} \approx 4.6$ eV) asymptotically. For the thinner Al layer, the dispersion curve deviates slightly farther from the resonance energy due to the strong interaction of SPP modes in the two interfaces. In fact, when the thickness of Al is 50 nm, the dispersion curve almost coincides with that of semi infinite thickness Al film. The dotted lines in Figs. 3(b)–3(d) are the SPP dispersion relation of AlGaN/Al/air structure, which is calculated by the formula[13]

$$\left(\frac{\gamma_1}{\varepsilon_1}+\frac{\gamma_2}{\varepsilon_2}\right)\left(\frac{\gamma_3}{\varepsilon_3}+\frac{\gamma_2}{\varepsilon_2}\right)-\left(\frac{\gamma_1}{\varepsilon_1}-\frac{\gamma_2}{\varepsilon_2}\right)\left(\frac{\gamma_3}{\varepsilon_3}-\frac{\gamma_2}{\varepsilon_2}\right)\mathrm{e}^{-2\gamma_2 t}=0,$$
$$(\gamma_i = k^2-\varepsilon_i\omega^2/c^2, \quad i=1,2,3). \tag{6}$$

Here ε_1, ε_2, and ε_3 are the permittivity of AlGaN, Al, and air, respectively. t is the thickness of Al film. It can be seen from the figure that the calculated results are basically consistent with the FDTD fitting result. That is to say, the influence of 3nm-thick Al_2O_3 on the dispersion relation of SPP can be ignored. It should be noted that since the imaginary part of wave vector k is difficult to obtain from FDTD simulation, we use the dispersion relation calculated by formula (6) when calculating the modified DOS of SPP mode. Figure 4 shows the modified DOS of SPP modes from the AlGaN/Al interface.

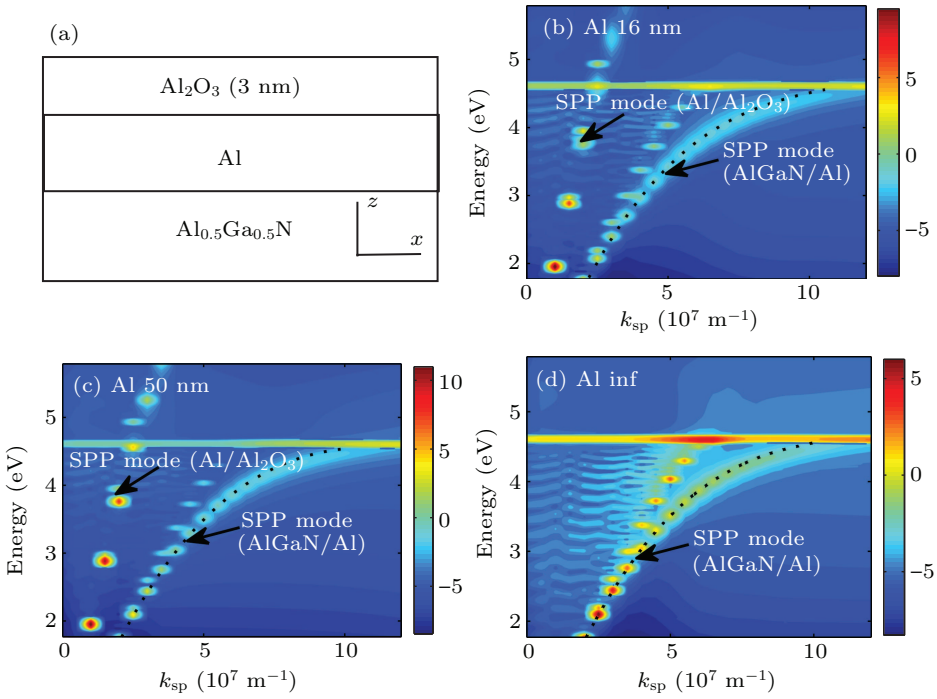


Fig. 3. (a) Schematic diagram of the $Al_{0.5}Ga_{0.5}N$/Al/Al_2O_3 slab structure and the dispersion relation of SPP modes with (b) 16 nm Al film, (c) 50 nm Al film, and (d) infinite thickness Al film.

For the $Al_{0.5}Ga_{0.5}N/Al/Al_2O_3$ slab with different Al thickness, the modified DOS of SPP mode has a maximum value at 4.4–4.48 eV. The energy corresponding to the peak DOS of SPP mode is lower than the SP resonance energy, which can be attributed to the larger imaginary part of the wave vector at the SP resonance. In addition, compared with other Al film thickness, the peak DOS of 50 nm thick Al film is relatively large.

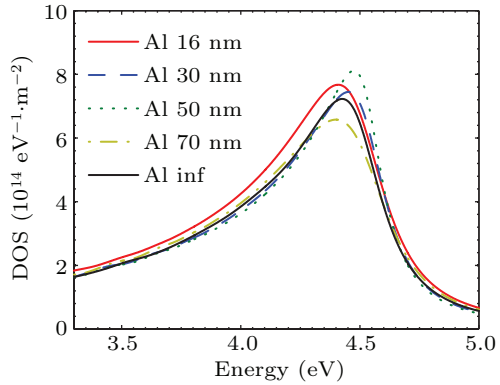


Fig. 4. The modified DOS from the AlGaN/Al interface for the $Al_{0.5}Ga_{0.5}N/Al/Al_2O_3$ slab with different Al thickness.

Figure 5 shows the normalized electric field (E_x, E_z) with infinite thickness Al film, 50 nm Al film, 30 nm Al film, and 16 nm Al film from 2D FDTD simulation. The dimension of the simulation range is 1 μm×2 μm for the z and x directions. The PML boundary conditions are set in the both directions. In order to eliminate the influence of "magnetic dipole" light source on detecting the electric field of SPP mode, a high absorption material is used to separate the light source from the monitor in the simulation. Only 4 nm gap are left to pass through the excited SPP mode from the AlGaN-Al interface. In Fig. 5(a), the normalized electric field solved analytically is also shown. The corresponding un-normalized electric field from the AlGaN–Al interface is calculated by the following formula:[18]

$$E_0 = \begin{cases} a_p \dfrac{q_{\mathrm{M}}}{\mathrm{i}\varepsilon_{\mathrm{M}}\omega} \mathrm{e}^{-q_{\mathrm{M}}z} \mathrm{e}^{\mathrm{i}(kx-\omega t)} \boldsymbol{e}_x \\ \quad + a_p \dfrac{k}{\varepsilon_{\mathrm{M}}\omega} \mathrm{e}^{-q_{\mathrm{M}}z} \mathrm{e}^{\mathrm{i}(kx-\omega t)} \boldsymbol{e}_z, \quad x > 0, \\ a_p \dfrac{-q_{\mathrm{D}}}{\mathrm{i}\varepsilon_{\mathrm{D}}\omega} \mathrm{e}^{q_{\mathrm{D}}z} \mathrm{e}^{\mathrm{i}(kx-\omega t)} \boldsymbol{e}_x \\ \quad + a_p \dfrac{k}{\varepsilon_{\mathrm{D}}\omega} \mathrm{e}^{q_{\mathrm{D}}z} \mathrm{e}^{\mathrm{i}(kx-\omega t)} \boldsymbol{e}_z, \quad x < 0 \end{cases}$$

with

$$q_{\mathrm{M}}^2 = k^2 - \mu\varepsilon_{\mathrm{M}}\omega^2, \quad q_{\mathrm{D}}^2 = k^2 - \mu\varepsilon_{\mathrm{D}}\omega^2. \tag{7}$$

Here, the subscripts M and D denote Al and AlGaN materials, respectively. From Fig. 5(a), it can be seen that the FDTD fitting result is basically consistent with the analytical solution result. In addition, the SPP evanescent field decays exponentially. It can be seen from the figure that the evanescent field on the AlGaN side is almost 0 at a distance of 50 nm from the metal aluminum. The short SP coupling distance will become the difficulty in the practical preparation of SP coupled LED devices. With the decrease of Al layer thickness, the field intensity on AlGaN side decreases obviously due to the coupling of SPP modes from the two interfaces of Al layer. At the same time, the influence of the light source on the detected field distribution is more significant, so that the evanescent field on the AlGaN side of the structure with Al thickness of 16 nm will not be exponentially reduced to 0, as shown in Fig. 5(d). Moreover, as Al thickness is decreased to 16 nm, it is also observed that the E_x component of the normalized electric field on the AlGaN side is greater than the E_z component, which means that the SE rate of TE polarization will be greater than that of TM polarization.

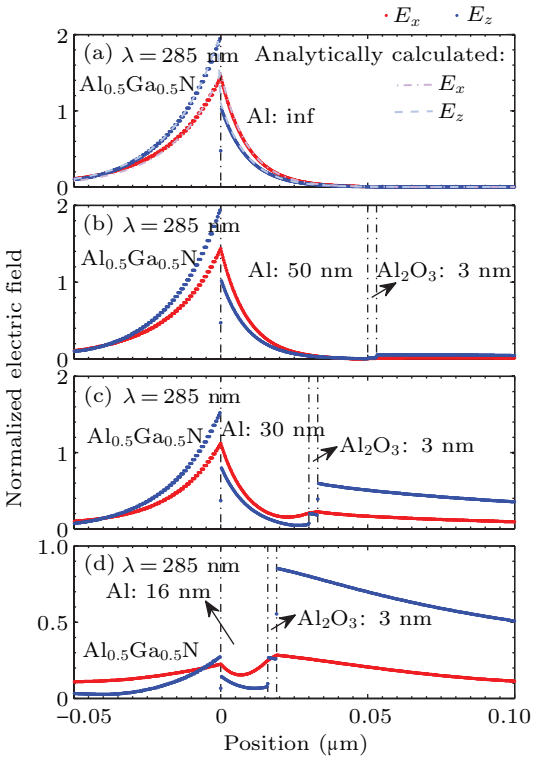


Fig. 5. The normalized electric field with (a) infinite thickness Al film, (b) 50 nm Al film, (c) 30 nm Al film, and (d) 16 nm Al film.

3.2. SE rate into SPP mode

By using the DOS and normalized electric field obtained above, the TE/TM polarized SE rate into the SPP mode is calculated. Here, the radiation dipole is considered to come from a quantum well structure composed of a 2 nm $Al_{0.35}Ga_{0.65}N$ well layer and an 8 nm $Al_{0.5}Ga_{0.5}N$ barrier layer. The band structure is calculated by the 6 × 6 K-P method. The sheet carrier density is set as 8×10^{12} cm^{-2}. Figure 6 shows the TE/TM polarized spontaneous emission spectra from the SP–QW coupling. The thickness of Al is set to be infinite. The spacing d between QW and Al is set to be 15 nm and 25 nm. Compared with the case without SP coupling, the SE rate into SPP mode

is significantly improved regardless of TE polarized emission or TM polarized emission. However, the degree of polarization (DOP) decreased from -14% without SPP coupling to -44% ($d = 15$ nm) and -42% ($d = 25$ nm). The DOP is defined as $\rho = (I_{\rm TE} - I_{\rm TM})/(I_{\rm TE} + I_{\rm TM})$. $I_{\rm TE}$ and $I_{\rm TM}$ are the integrated intensity of the TE-polarized and TM-polarized SE rate into SPP mode or free space.

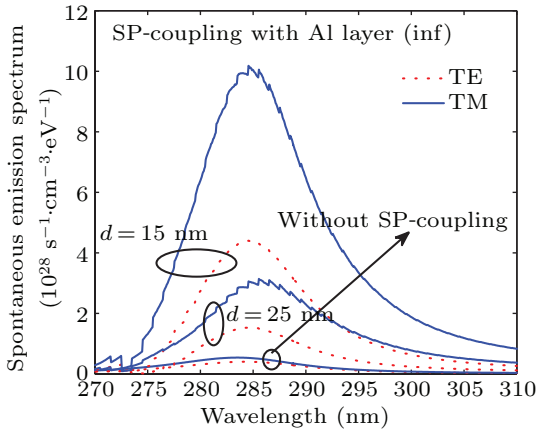


Fig. 6. TE/TM polarized spontaneous emission spectra from the SP–QW coupling. The thickness of Al is set to infinite. The spacing d between QW and Al is set to be 15 nm and 25 nm. The spontaneous emission spectrum without SP coupling is also shown.

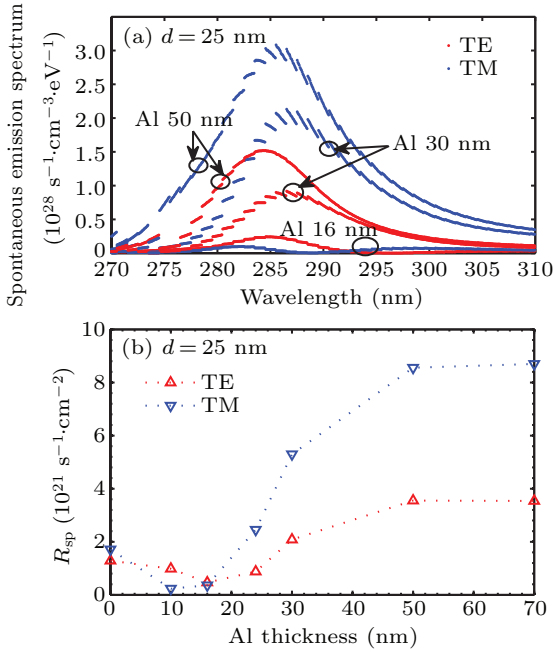


Fig. 7. (a) TE/TM polarized spontaneous emission spectra from SP coupling with Al thickness of 16 nm, 30 nm, and 50 nm; (b) the TE/TM polarization total SE rate ($R_{\rm sp}$) into SPP mode as a function of Al thickness. The $R_{\rm sp}$ into free space without SP coupling is also shown in (b).

Since the normalized electric field intensity obviously depends on Al thickness, the SE rate into SPP mode will change significantly with the change of Al thickness. Figure 7(a) shows the TE/TM polarized spontaneous emission spectra from SP coupling with Al thickness of 16 nm, 30 nm, and 50 nm. With the decrease of Al thickness from 50 nm to 16 nm, the SE rate into SPP mode decreases significantly in both TE mode and TM mode. In particular, as Al thickness is 16 nm, TE polarization emission is greater than TM polarization emission, which is different from the other two cases. For SP coupling with Al thickness of 16 nm, 30 nm and 50 nm, the calculated degrees of polarization are 13%, -44% and -41%, respectively. Figure 7(b) shows the TE/TM polarization total SE rate ($R_{\rm sp}$) into SPP mode as a function of Al thickness. The total SE rate can be obtained by $R_{\rm sp} = L_z \int_0^\infty r_1^{\rm spon}(\hbar\omega)\mathrm{d}\hbar\omega$. It can be observed that for SP coupled LEDs with Al thickness less than 16 nm, the TE polarization emission is greater than that of TM polarization. Nevertheless, the total spontaneous emission rate is significantly smaller than that without SP coupling structure. Only when the thickness of Al layer is greater than 24 nm, the average total spontaneous emission rate is greater than that without SP coupling.

3.3. Transmittance for Al NP structure

It is shown above that the DOP of SP coupled LED varies with Al thickness. However, due to the anisotropic extraction behavior of polarized light,[19] the actual DOP will be different from the above calculation results. Figure 8(a) shows the transmission spectra of an Al NP placed on the $Al_{0.5}Ga_{0.5}N$ layer. The structure diagram of the simulation is shown in Fig. 1. It can be obviously observed that the transmittance of TE-polarized light is much larger than that of TM-polarized light, which will lead to greater DOP. Compared with the case without SP coupling, the ratio of transmittance between TE polarization and TM polarization through SP coupling is significantly improved. Figure 8(b) shows the transmittance as a function of Al thickness at $\lambda = 285$ nm. When the thickness of Al is less than 20 nm, the transmittance of TM polarization decreases significantly faster than that of TE polarization with the increase of Al thickness. When the thickness of Al is greater than 20 nm, the transmittance of both TE/TM polarizations basically remains unchanged with the increase of Al thickness. With the increase of Al thickness from 0 nm to 70 nm, the ratio of transmittance between TE polarized emission and TM polarized emission increases from 1.2 to 7.8. It should be noted that the position of radiation dipole can significantly affect the calculated TE/TM polarized light transmission ratio. For example, when the dipole moves from directly below Al NP to the edge, the ratio for the 30 nm Al NP structure decreases from 7.5 to 1.82. Nevertheless, the ratio of average transmittance of TE/TM polarized light can still reach 3.06. As a result, the DOP of SP coupled LED can be expected to be improved in the actual applications, as reported in Ref. [11].

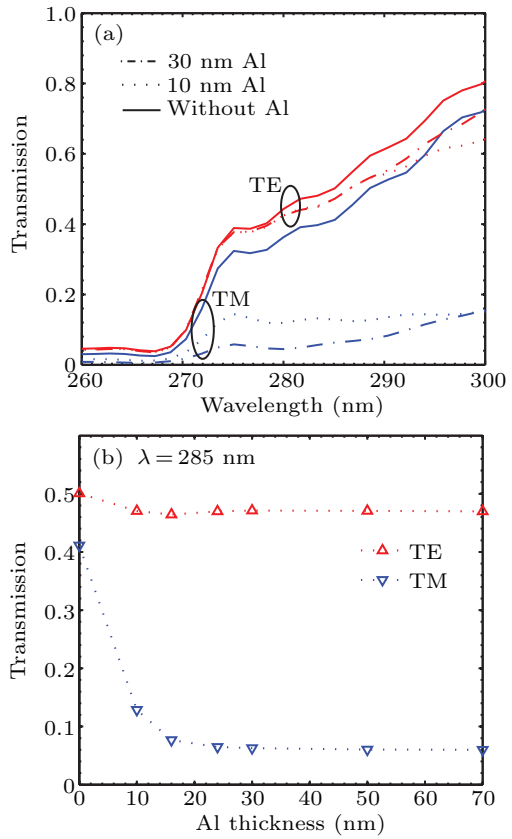


Fig. 8. (a) The transmission spectra of an Al NP placed on the $Al_{0.5}Ga_{0.5}N$ layer; (b) the transmittance as a function of Al thickness at $\lambda = 285$ nm.

4. Conclusion

In summary, the optical anisotropy of SP coupled LED is studied by 6×6 K-P method and FDTD simulation. Through SP coupling, the energy of the radiation dipole can be transferred to the SPP mode, which can be expected to improve the radiation recombination rate of LED devices. However, the dipole-SP coupling has different effects on TE/TM polarized emission. For the $Al_{0.5}Ga_{0.5}N/Al/Al_2O_3$ slab structure, when the thickness of Al is less than 16 nm, the TE-polarized SE rate into SPP mode is significantly higher than that of TM mode due to the larger E_x component of the normalized electric field on the AlGaN side. At the same time, when Al thickness is greater than 24 nm, TM polarized emission becomes the dominant emission, and the average total SE rate is greater than that without SP coupling. For the Al NPs structure, the extraction behavior of TE/TM polarized light is obviously different. Compared with the structure without Al, the decrease of transmittance of TM polarized light is much greater than that of TE polarized light. Thus, the ratio of transmittance between TE polarization and TM polarization for the 30 nm Al NP structure can be increased by 1.55 times at $\lambda = 285$ nm. In practical application, the reasonable design of SP coupled LED device can significantly improve the DOP and luminous efficiency.

Acknowledgements

This work was supported by the National Nature Science Foundation of China (Grant Nos. 62004109, 61874168, and 62074086), Jiangsu Provincial Double-Innovation Doctor Program, Development of antibacterial multifunctional PVC facing new material technology (Grant No. 21ZH626).

References

[1] Amano H, Collazo R, Santi C D, Einfeldt S, Funato M, Glaab J, Hagedorn S, Hirano A, Hirayama H, Ishii R, Kashima Y, Kawakami Y, Kirste R, Kneissl M, Martin R, Mehnke F, Meneghini M, Ougazzaden A, Parbrook P J, Rajan S, Reddy P, R?mer F, Ruschel J, Sarkar B, Scholz F, Schowalter L J, Shields P, Sitar Z, Sulmoni L, Wang T, Wernicke T, Weyers M, Witzigmann B, Wu Y R, Wunderer T and Zhang Y 2020 *Physica D* **53** 503001

[2] Takano T, Mino T, Sakai J, Noguchi N, Tsubaki K and Hirayama H 2017 *Appl. Phys. Express* **10** 031002

[3] Nagasawa Y and Hirano A 2018 *Appl. Sci.* **8** 1264

[4] Chang W Y, Kuo Y, Yao Y F, Yang C C, Wu Y R and Kiang Y W 2018 *Opt. Express* **26** 8340

[5] Li Y, Zhu Y, Mei G, Wang M, Deng H and Yin H 2020 *Jpn. J. Appl. Phys.* **59** 084001

[6] Khan M A, Maeda N, Jo M, Akamatsu Y, Tanabe R, Yamada Y and Hirayama H 2019 *J. Mater. Chem. C* **7** 143

[7] Wang Y, Rong X, Ivanov S, Jmerik V, Chen Z, Wang H, Wang T, Wang P, Jin P, Chen Y, Kozlovsky V, Sviridov D E, Zverev M, Zhdanova E, Gamov N, Studenov V, Miyake H, Li H, Guo S, Yang X, Xu F, Yu T, Qin Z, Ge W, Shen B and Wang X 2019 *Adv. Opt. Mater.* **7** 1801763

[8] Guo W, Sun H, Torre B, Li J, Sheikhi M, Jiang J, Li H, Guo S, Li K H, Lin R, Giugni A, Di Fabrizio E, Li X and Ye J 2018 *Adv. Funct. Mater.* **28** 1802395

[9] Lee J W, Ha G, Park J, Song H G, Park J Y, Lee J, Cho Y H, Lee J L, Kim J K and Kim J K 2020 *Acs Appl. Mater. Interfaces.* **12** 36339

[10] He J, Wang S, Chen J, Wu F, Dai J, Long H, Zhang Y, Zhang W, Feng Z C, Zhang J, Du S, Ye L and Chen C 2018 *Nanotechnology.* **29** 195203

[11] Zhang C, Tang N, Shang L, Fu L, Wang W, Xu F, Wang X, Ge W and Shen B 2017 *Sci. Rep.* **7** 2358

[12] Li Y, Zhang R, Xie Z, Liu B, Chen P, Zhang G, Tao T, Zhuang Z, Zhi L, Gan T and Zheng Y 2013 *J. Appl. Phys.* **114** 113104

[13] Neogi A, Lee C W, Everitt H O, Kuroda T, Tackeuchi A and Yablonovitch E 2002 *Phys. Rev. B* **66** 153305

[14] Feng X, Cui K, Liu F and Huang Y 2012 *Appl. Phys. Lett.* **101** 121102

[15] Chuang S L and Chang C S 1997 *Semicond. Sci. Technol.* **12** 252

[16] Takeuchi K, Adachi S and Ohtsuka K 2010 *J. Appl. Phys.* **107** 023306

[17] Maier S A 2007 *Plasmonics: fundamentals and applications* (New York: Springer) p. 28

[18] Khurgin J B, Sun G and Soref R A 2007 *J. Opt. Soc. Am. B* **24** 1968

[19] Wang H, Fu L, Lu H M, Kang X N, Wu J J, Xu F J and Yu T J 2019 *Opt. Express* **27** A436